THE JOURNAL OF PHYSICAL CHEMISTRY C

C: Surfaces, Interfaces, Porous Materials, and Catalysis

Benzene Adsorption on Rh(111): A New Perspective on Intermolecular Interactions and Molecular Ordering

Michael-John Treanor, Jose Antonio Garrido Torres, Catherine J. Bromley, Herbert A Fruchtl, and Renald Schaub

J. Phys. Chem. C, **Just Accepted Manuscript** • DOI: 10.1021/acs.jpcc.8b02798 • Publication Date (Web): 07 May 2018

Benzene Adsorption on Rh(111): A New Perspective on Intermolecular Interactions and Molecular Ordering

Michael-John Treanor, José A. Garrido Torres, Catherine J. Bromley, Herbert A. Früchtl, Renald Schaub*

EaStCHEM and School of Chemistry, University of St Andrews, St Andrews, KY16 9ST, United Kingdom

* Corresponding author: Dr Renald Schaub, renald.schaub@st-andrews.ac.uk

** The research data supporting this publication can be accessed at:

10.17630/97b7cdbd-2ed6-4bbe-8569-34de85dc60dd

Abstract

The adsorption of benzene on the Rh(111) substrate was investigated through scanning tunneling microscopy (STM) imaging and density functional theory (DFT) calculations. Experiments were carried out at various surface coverages, with the amount of benzene adsorbed determined to influence the molecular adsorption site, the intermolecular interactions, and the interaction between the molecule and the substrate. At a sub-monolayer coverage of the surface, the molecules are disordered and kept apart by a strong inter-adsorbate repulsion, with a preference for the molecule to adsorb on a three-fold hcp hollow site. At high coverage, the preferred adsorption site becomes the two-fold symmetric bridge site, whether as part of the two dense ordered structures that form at high coverage ((2√3×3)*rect* or

(√19×√19)R23.4°) or as part of the disordered array of benzene molecules, which are arranged in formations which resemble the "building blocks" of the ordered overlayers. Despite the adsorption energy for benzene within both dense structures being similar, the (√19×√19)R23.4° overlayer is only observed if the substrate is annealed to 363 K during or after deposition, indicating that the formation of the (√19×√19)R23.4° ordering is inhibited by an activation barrier at lower temperatures and can only be overcome by increasing the temperature of the Rh(111) support.

Introduction

As the smallest possible aromatic hydrocarbon molecule, the adsorption of benzene on transition metal substrates has been extensively studied in surface science, serving as an appropriate model for the interaction of a π-conjugated system with metal surfaces[1–13]. This is a subject of broad interest, not only on a fundamental level but in applied research as well. Previous investigations were motivated by financial and environmental concerns in heterogeneous catalysis; for example, the concentration of aromatic species in diesel fractions had a negative impact on the fuel quality while also resulting in problematic emissions present in the exhaust gas[14–17]. Modern research is focused on the application of aromatic molecules in devices such as photovoltaic cells[18], field-effect transistors[19] and organic light-emitting diodes (OLEDS)[20]. Establishing a better understanding of the π-metal interaction on various surfaces is crucial to the development and optimization of such devices.

Various properties of the benzene-substrate interaction have been determined to be common across different metal surfaces. Almost all surfaces studied have demonstrated that benzene adsorbs with the plane of the aromatic ring parallel to the plane of the substrate[1,2,7,10,21–23]. The strength of the bonding between benzene and transition metal surfaces follows the general trend of reactivity across the periodic table[24], with the molecule binding weakly via physisorption to coinage metals[25–27] and strongly via chemisorption to more catalytic surfaces[4,24,25]. A variety of surface science techniques have been used to determine these properties, as well as others such as the binding energy, across numerous metal surfaces, including HREELS[28], LEED[29], TPD[30], ARUPS[31], XPS[32] and NIXSW[33].Spectroscopic techniques have also been employed to obtain microscopic information about the commensurability of the structures that benzene forms on different catalytic substrates[34–37]. In more recent years, theoretical studies have been preferred for the study of the adsorption characteristics of benzene on various metals[27,38–45]. The molecular self-organization of benzene on these surfaces is thermodynamically driven by competing interactions: (1) the repulsive interactions between the benzene molecules, and (2) the attractive metal-molecule interactions. Consequently, variations in surface coverage result in the formation of different morphologies of molecular ordering as a direct result of the competition between these interactions [46–48].

Benzene adsorption has been extensively studied on the surface of the Rh(111) single crystal[21,29,30,37,49–55], with a significant amount of attention given to the behavior of benzene upon coadsorption with CO. This is in part due to the difficulty in preparing such a reactive surface free of typical UHV pollutants such as CO. Upon realizing that the

initial studies of benzene on Rh(111) involved coadsorbed structures with CO, research interest changed to how these different molecules interacted with one another on a catalytic substrate. As a result of benzene and CO having oppositely orientated dipoles upon binding to the substrate, a strong attractive interaction occurs[56] which induces two possible ordered overlayers: a (3×3) structure with one benzene and two CO molecules per unit cell, and a *c*(2√3×4)*rect* structure with one benzene and one CO per unit cell[50–52]. The formation of these ordered overlayers is dependent on the deposition conditions, with both molecules determined to adsorb on hexagonally close-packed (hcp) hollow sites irrespective of the way the molecules are ordered. STM images, mainly of the (3×3) ordering, have confirmed the hcp adsorption for the benzene molecules through their appearance in these images as three-lobed structures[57], in agreement with simulated STM images for benzene on hcp sites on Rh(111)[58]. The ordering of benzene upon coadsorption with CO has also been observed on other transition metal surfaces such as Pt(111)[45,52,59], Pd(111)[9,55], and Co(0001)[60,61]. The same phenomenon has also been reported for benzene coadsorbed with other molecules, particularly electronegative ones such as oxygen and NO[62,63].

Unlike the benzene/CO coadsorbed system described above, the adsorption of just benzene on Rh(111) does not feature an attractive interaction between the adsorbates. Without CO, benzene ordering has only been observed upon saturation of the surface with the molecules. This results in the self-organization of the molecules into two different commensurate nanostructures. A (2√3×3)*rect* ordering (relative coverage of Θ_{C6H6}= 0.166), with two benzene molecules per unit cell (all adsorbed on bridge sites), was first identified through LEED patterns[52], which also suggested the ordering was

short-ranged. HREELS experiments revealed two out-of-plane C-H bending modes for the benzene molecule, leading to the determination of benzene adsorbed on a three-fold hollow site in the disordered regions[52]. Another dense structure has been identified through LEED and ARUPS to form upon annealing a benzene saturated Rh(111) surface to 363 K. This structure, with relative coverage of Θ_{C6H6}= 0.159, contains three benzene molecules per unit cell. Although this was not experimentally proven, it was proposed that the molecules in this arrangement also adsorb onto bridge sites. This structure has been designated as a (√19×√19)R23.4° overlayer[31].

Previous studies have acquired STM images of benzene on Rh(111) for the benzene/CO coadsorbed system as well as the (2√3×3)*rect* pure benzene ordering[36,37,57]. However, there has not been any direct observation of the (√19×√19)R23.4° overlayer, either through STM imaging or otherwise. All investigations involving pure benzene adsorption on Rh(111) have been limited to the case of saturated coverage, thus the structural evolution of benzene upon varying coverage, as well as the temperature of the substrate, is poorly understood.

This paper presents a study on the adsorption of pure benzene on Rh(111), from low coverage resulting in isolated molecules, to high coverage with densely packed overlayers. The phenomena that dictates the behavior of benzene on the Rh(111) surface shall be investigated directly through low temperature UHV-STM measurements. These measurements are performed in conjunction with a comprehensive theoretical investigation using DFT calculations to qualitatively rationalize the adsorption characteristics of benzene on the Rh(111) surface.

Methods

All STM measurements were performed in a UHV microscope chamber with a low temperature CreaTec STM. The Rh(111) single crystal was cleaned in a conjoining preparation chamber via repeated cycles of Ar^+ sputtering followed by a subsequent anneal above 970 K in oxygen (up to 1×10^{-6} mbar) for five minutes and then a further ten minutes under recovering vacuum. Benzene was purified through multiple pump-freeze-thaw cycles and the deposition of the molecules onto the Rh(111) surface was carried out under excellent vacuum conditions (i.e. a base pressure of $\leq1\times10^{-10}$ mbar) to avoid CO contamination. The benzene dosing system was also constantly refreshed to keep it free from CO. Various amounts of benzene were deposited over the course of these experiments, ranging from 0.1 L to 20 L. All images were acquired at approximately 5 K.

Periodic DFT calculations were performed using the projector-augmented-wave (PAW)[64,65] method as implemented in the Vienna ab-initio simulation package (VASP)[66,67]. Valence electrons were described using plane-waves, with their basis sets expanded up to a 400 eV kinetic energy cut-off. The rhodium surface along the (111) direction was modelled via a four-layer slab (with the two upper layers relaxed during optimization) and a vacuum gap between periodic images of 15 Å. The integration of the Brillouin zone was sampled using various k-point grids, reflecting the varying dimensions of the surface and benzene coverage i.e. 7×7×1 for the smaller unit cells used, (3×3) and (4×4), 5×5×1 for the (5×5) and (6×6) unit cells and 3×3×1 for the (7×7) and (8×8) unit cells. The molecules in the gas phase were modelled in a cubic cell (lattice parameter of 30 Å) considering only the Γ-point. Geometry optimizations

were converged when the residual forces of all the atoms were smaller than 0.02 eV/Å. The electronic convergence threshold was set to 10^{-5} eV.

Various functionals were employed to calculate the adsorption energy of benzene on the modelled Rh(111) surface, using the formula:

$$E_{ads} = E_{Bz/Rh(111)} - E_{Rh(111)} - n \times E_{Bz(gas)}$$

Where E_{ads} is the adsorption energy of a given system and $E_{Bz/Rh(111)}$ is the energy of the system when n molecules of benzene are adsorbed onto the metal slab. Also, $E_{Bz(gas)}$ refers to the energy of benzene in the gas phase while $E_{Rh(111)}$is the energy of the slab. Adsorption energies per molecule are acquired by dividing the calculated adsorption energy by the number of benzene molecules (n) included in the unit cell, while adsorption energies per unit area are obtained by dividing the adsorption energy by the unit cell area occupied at the specific coverage being modelled. These values are not normalized by the number of molecules within the unit cell to allow for the comparison of results for the different overlayers investigated. Finally, constant height STM simulations were calculated with the use of the Tersoff-Hamann approximation[68,69].

Results and Discussion

A. Low coverage of benzene

Previous theoretical investigations have established that the two most energetically favorable adsorption sites for benzene on (111) transition metal surfaces have the center of the molecule positioned either above an hcp site or a bridge site[33,39,70]. When adsorbed on the hcp site, the benzene molecule is arranged in such a way that the C-C

bonds of the molecule are aligned with the high symmetry directions of the substrate, while the bonds are rotated ±30° with respect to the atomic rows of the substrate when benzene adsorbs onto a bridge site. As such, these adsorption arrangements are referred to as hcp0° and bridge30° throughout this paper.

STM images were acquired of benzene on Rh(111) at low (i.e. below saturation) coverage of the substrate, revealing that the molecules neither order nor pair up/cluster together under such conditions. Instead, each benzene is isolated from its nearest neighbors by several Angstroms. The molecules were deposited onto the substrate at 150 K, room temperature and 363 K, with no discernible differences in the ordering of the molecules observed in the STM measurements.

As shown in Figure 1, high-resolution images were acquired at constant height after depositing 0.6 L of benzene with the substrate at room temperature to ascertain the adsorption site of the molecules at this coverage. After deposition, the sample was subsequently cooled to approximately 5 K, thereby ensuring that thermal equilibrium was reached. The image in Figure 1a reveals the benzene molecules as hexagonal protrusions on the surface, while the image in Figure 1b resolves the atomic corrugation of the Rh(111) surface as well as the benzene molecules themselves. The visualization of the rhodium atoms in Figure 1b allows for the construction of a lattice grid that represents the Rh(111) translational periodicity, which in turn is used to elucidate the adsorption site of the benzene molecules on the surface, as seen in Figures 1c and 1d.

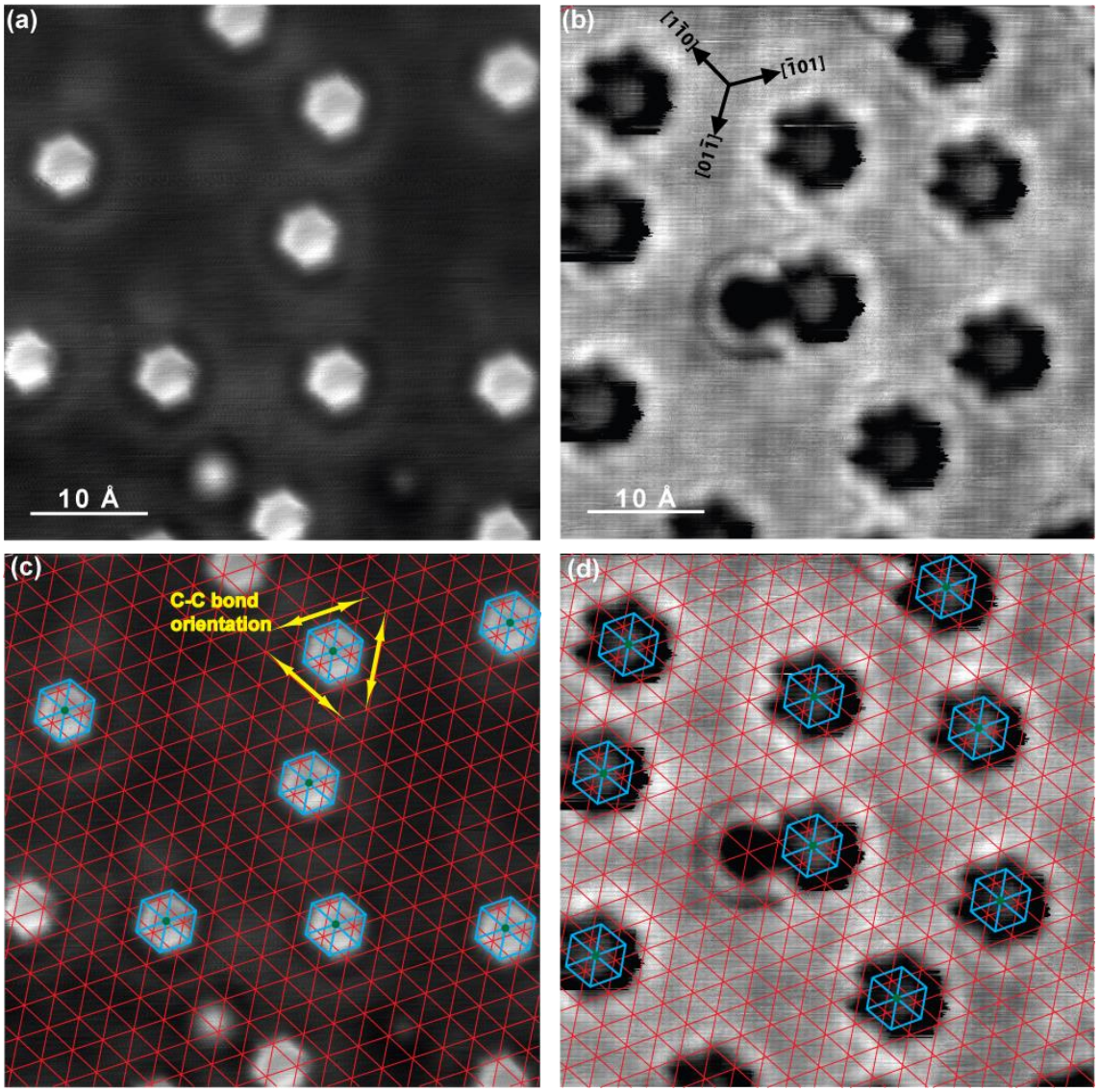

Figure 1(a) 46×47 Å^2 constant height image of benzene deposited on Rh(111). (b) 46×47 Å^2 constant height image of benzene on Rh(111) with atomic resolution. The atomic resolution was used to create a Rh(111) lattice grid, which, when applied to the images as shown in (c) and (d), demonstrates that the molecules are all adsorbed onto three-fold symmetric hollow sites. The bias applied in both images was 26 mV.

The clear hexagonal structure of the benzene molecule in Figure 1a and the application of the lattice grid in Figure 1c makes it clear that the C-C bonds are aligned with the high symmetry direction of the substrate i.e. the molecules are oriented 0° with respect to the surface. The lattice grid, which is pinned onto the rhodium top sites in Figure 1d, also leads to the determination that the molecules are all adsorbed onto a three-fold

hollow site. The exact hollow site can be determined experimentally by identifying a triangular vacancy defect, a regularly observed feature on Rh(111) surfaces where several atoms in the top layer are missing, forming a void in the shape of a triangle. If this defect can be observed in an STM image with the atoms of the first and second layer resolved, as shown in Figure 2, then it is possible to distinguish between the two types of hollow sites, hcp and fcc.

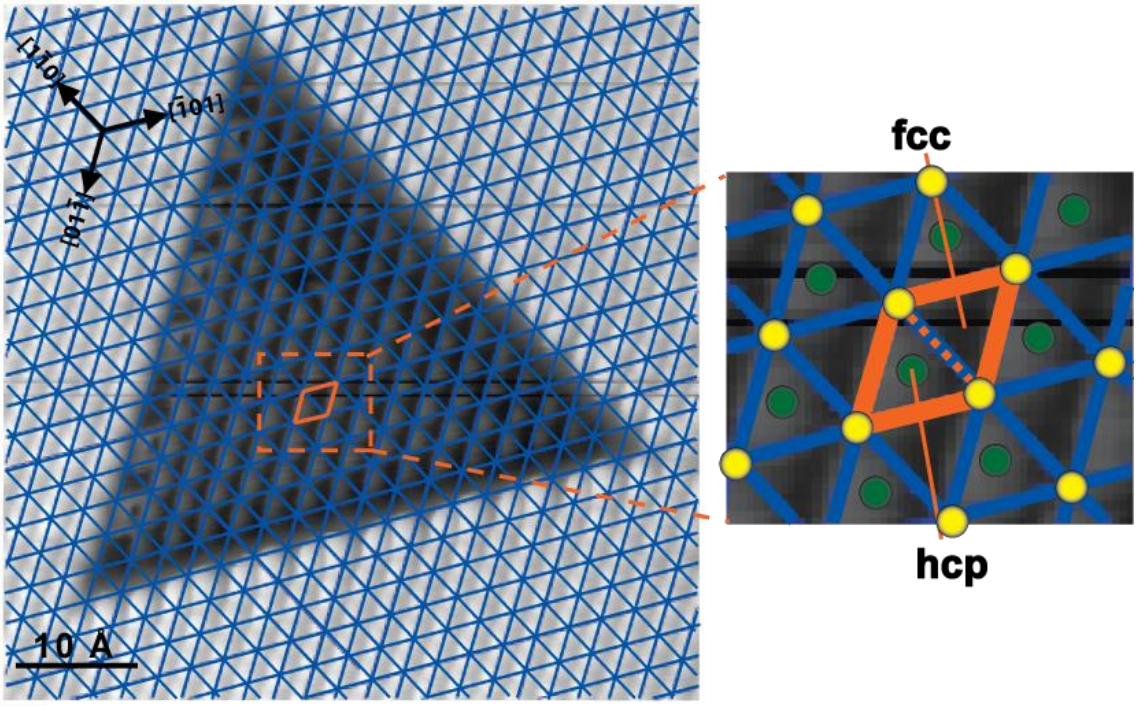

Figure 2 STM image of a triangular vacancy defect on Rh(111) with atomic resolution. The blue grid represents the Rh(111) lattice with respect to the top layer. The zoomed in part of the image highlights the position of the atoms in the top layer (yellow circle) and the layer directly beneath (green circles).

The blue grid in Figure 2 represents the lattice of the rhodium atoms on the top layer, while the orange rhomboid is used to highlight a single unit cell of the Rh(111) surface. This unit can be split into two triangles with one of the two hollow sites at the center of them. As this image provides the position of the atoms in the second layer, it can be concluded that the triangular half unit cell that represents the hcp site is aligned parallel

with the triangular vacancy, while the other half cell that represents the fcc site is aligned anti-parallel with the defect. Using this information, we can confirm that the benzene molecules deposited on Rh(111) at low coverage as shown in Figure 1 adsorb onto the surface in the hcp0° configuration.

The adsorption of benzene onto the hcp hollow site at low coverage is somewhat surprising, given that the bridge30° configuration was determined via theoretical calculations to be the most stable adsorption arrangement for benzene on Rh(111)[71]. However, these calculations were performed using a (3x3) unit cell to represent the benzene on the Rh(111) surface, which does not completely and accurately describe what is observed in these experiments. The calculations do suggest that the difference in adsorption energy for the two most stable configurations, bridge30° and hcp0°, is minimal, with some methods producing a difference as low as 10 meV. As benzene is not observed to adsorb onto bridge30° sites after deposition onto the Rh(111) crystal held at room temperature, then in reality it is the bridge30° configuration that is less stable (with the hcp0° the experimentally observed adsorption site). To confirm this hypothesis, benzene was deposited at the same coverage seen in Figure 1 but with the substrate maintained at around 150 K during the deposit. This was carried out as depositing at lower temperatures limits the molecular diffusion that has previously been observed to occur with benzene on Rh(111) at room temperature[37]. The result of this is shown in Figure 3.

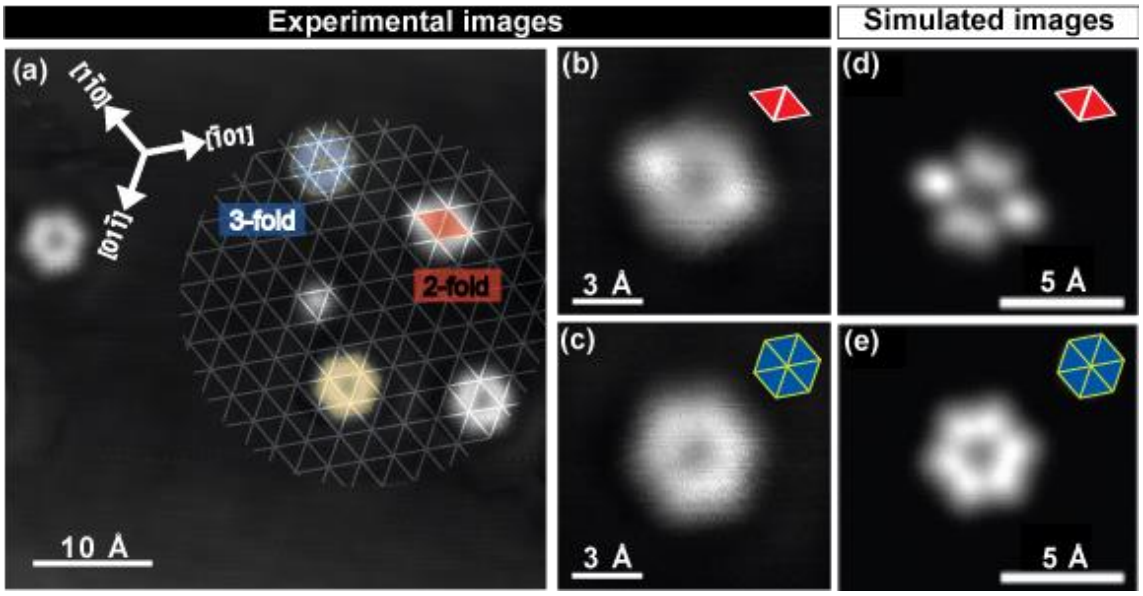

Figure 3(a) 46×47 Å^2 constant height STM image (V = 52 mV) of benzene deposited onto Rh(111) while the sample was cooled to approximately 150 K. A Rh(111) lattice grid is placed on the image to highlight the different adsorption sites observed. A blue hexagon is used to highlight a molecule in a three-fold hollow site and a red parallelogram for a molecule on a two-fold bridge site. A yellow hexagon highlights a molecule on the other hollow site compared to the other molecules in the image. (b) and (c) provide a closer look at the distinct electronic contrast for the benzene molecules on the different sites. These images are compared to DFT-simulated images acquired with the same voltage parameters. Benzene in a bridge30° configuration, simulated in (d), compares favorably with (b), while the simulated image for hcp0° in (e) compares favorably with (c).

The high-resolution constant height image shown in Figure 3a allows for the visual distinction between benzene molecules adsorbed onto different sites. The dependence of the topographic appearance of an adsorbate on its adsorption site is a well-known phenomenon of STM imaging first identified with benzene on Pt(111)[12]. Most of the molecules appear identical to the feature highlighted by the blue hexagon in Figure 3a, which in turn resembles the hexagonal protrusions in Figure 1. Looking closer at the image in Figure 3a, it is clear that the edges of the hexagon are comprised of three lobes of bright contrast, a feature first identified for benzene adsorbed in the hcp0° configuration on Rh(111) in past STM measurements carried out on the coadsorbed

benzene/CO system[57]. In contrast, one molecule in the image appears elongated, with two protrusions located on opposing sides of the molecule, resulting in a distorted hexagonal appearance (and is highlighted by the red parallelogram in Figure 3a). Placing a Rh(111) lattice grid on the image confirms that the hexagonal protrusions are adsorbed onto hollow sites, while the distorted hexagon feature is centered over one of the three degenerate bridge sites. Interestingly, the hexagonal protrusions are centered over the same type of hollow site as the benzene molecules observed in Figure 1d (which have already been determined to be hcp hollow sites) with the exception of the protrusion marked by the yellow hexagon. It follows then that this molecule is adsorbed onto an fcc hollow site in a fcc0° configuration. The ability to visually distinguish between benzene adsorbed on bridge sites and hollow sites will be used in the next section.

The experimental and DFT-simulated images in Figure 3b-e provide further clarification on the types of adsorption sites that benzene adsorbs onto under these conditions. The images in Figure 3d and 3e were simulated for the optimized bridge30° and hcp0° configurations respectively. These simulated features are an excellent match to the experimental images of benzene in these two different adsorption sites, with the bridge30° simulated image matching the distorted hexagonal protrusion (Figure 3b) while the hcp0° image matches the regular hexagonal protrusion (Figure 3c). However, it is very difficult to experimentally distinguish between benzene adsorbed onto the hollow sites based on their electronic contrast alone and we are only able to do so here with the knowledge of the atomic positions in the second layer acquired from Figure 2. Statistical analysis of the images acquired after the low temperature (150 K) deposit reveals that around 81% of the benzene molecules can be assigned to the presumed hcp

hollow site, 13% are assigned to bridge sites and 6% are on the other hollow site, fcc. Once again, the molecules are determined to be adsorbed predominantly on hcp sites, with a small percentage in bridge sites and an even smaller percentage in fcc sites. This also confirms that the unique topographic signature for benzene is dependent on the symmetry of the adsorption site.

This experiment confirms that the two-fold bridge site is less stable than the three-fold hcp hollow site for benzene deposited onto Rh(111) at low coverages, although the observation of molecules on other sites indicates the difference in adsorption energy is small, as suggested by past theoretical investigations[71]. There was no indication of benzene adsorption on bridge sites when the deposit was carried out at room temperature or at 363 K; this is likely due to the diffusivity of benzene on the Rh(111) surface at such temperatures, with the thermal energy provided to the molecule at room temperature and above enough to allow for the relaxation of the molecules into the most stable arrangement (adsorbed onto the hcp site). By performing the deposit at lower temperature, the molecular diffusion that occurs at room temperature is at least somewhat quenched, therefore the thermalisation of the benzene/Rh(111) system is incomplete. This also explains the small percentage of benzene determined to adsorb in the fcc0° configuration after a low temperature deposit.

In tandem with our experimental work, the adsorption of benzene on both hcp and bridge sites on the Rh(111) surface was modelled, with the results compared to our STM results and the previous theoretical investigations. Four different functionals were used for comparison while also varying the size of the unit cell from (3×3) to (8×8) in an attempt to determine the qualitative impact of the intermolecular distance between

benzene molecules on their adsorption onto the substrate. The results from these calculations were plotted to show the adsorption energy versus the unit cell size determined through each method used as seen in Figure 4.

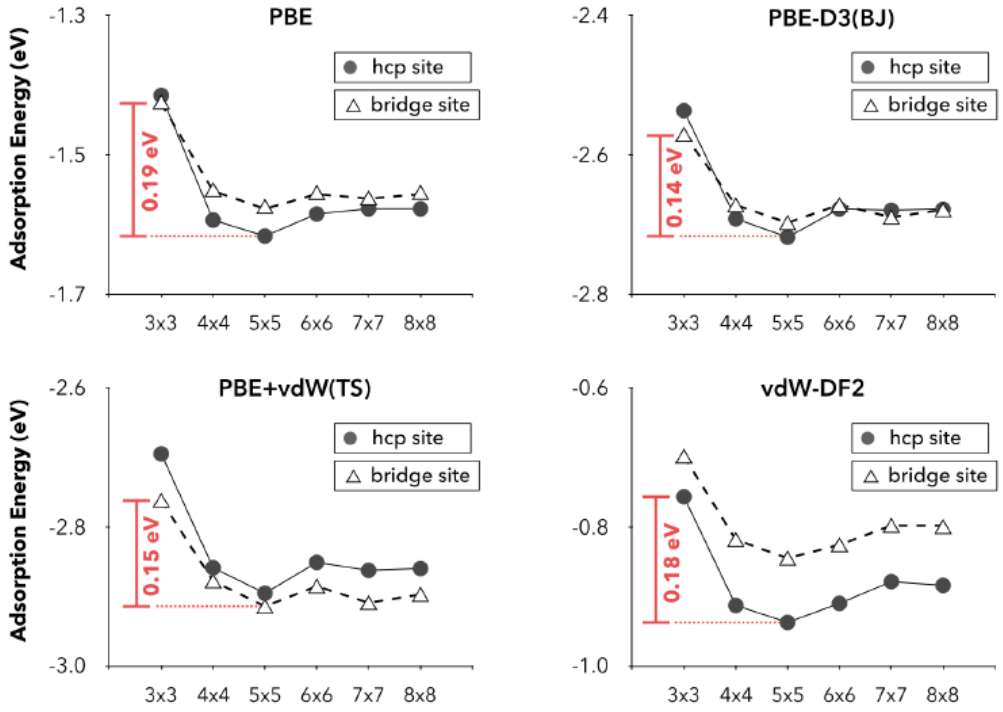

Figure 4 Plots of the calculated adsorption energies for benzene on hcp sites and bridge sites versus increasing cell size using the PBE, PBE-D3(BJ), PBE+vdW(TS) and vdW-DF2 functionals. The energy differences between the most stable adsorption sites for the (3×3) and the (5×5) unit cells are displayed in each plot.

By examining the plots in Figure 4, it is clear that, no matter the functional used, the most favorable adsorption values are found at a cell size of (5×5), while a severe energy penalty was observed upon decreasing the cell size down to (3×3). The lowest energy variation from the most stable adsorption site in the (5×5) unit cell to the most stable site in the (3×3) cell is observed with the PBE-D3(BJ) functional, but there is still a substantial energy cost of around 140 meV. The large increase in energy observed by moving to the (3×3) cell is indicative of the strong effect that the intermolecular repulsion between benzene molecules has at short range on the adsorption of benzene

on the Rh(111) surface. This coincides with the lack of pairing or clustering of molecules observed in the experimental STM images in Figures 1 and 3. This repulsive interaction at short inter-adsorbate distances is the opposite of what is observed upon coadsorption of benzene and CO on Rh(111). The structures that form upon coadsorption of these molecules[50,52] are a result of an attractive interaction between the opposing oriented dipoles of CO and benzene on the Rh(111) surface[56]. The repulsion observed upon pure benzene deposition is a result of the dipoles of the adsorbates all being oriented in the same direction.

As the (5×5) unit cell seems to provide the best comparison with the experimental results (at least in terms of the average intermolecular distance observed in the STM experiments discussed previously), it is best to focus the discussion on the data acquired when using this model. Table 1 reveals the computed adsorption energies for benzene on the two different adsorption sites for the (5×5) unit cell, as well as the energy difference between both sites for each functional. The energy difference is calculated by subtracting the energy of the system where the molecules are adsorbed on bridge sites from the energy of the system with the molecules on hcp sites, therefore a positive result indicates that bridge site adsorption is energetically favored. Corrected zero-point energy (ZPE) differences were also calculated for comparison with the uncorrected results, using the equation;

$$\Delta E_{hcp-bridge}(ZPE) = \Delta E_{hcp-bridge} + \frac{1}{2}h\sum_{i}(v_i^{hcp} - v_i^{bridge})$$

Where $\Delta E_{hcp-bridge}$ is the uncorrected energy difference between the adsorption energies for benzene on hcp and bridge sites while v_i^{hcp} and v_i^{bridge} are the respective

energies of the i-th vibrational mode for benzene when adsorbed on hcp and bridge sites. Without any reported experimental adsorption values for benzene on Rh(111), it is impossible to discuss the accuracy of each method used in a quantitative manner based on the computed adsorption energies. Instead, the quality of the methods will be discussed by analyzing the relative energies of the two most stable adsorption sites.

Methods	Adsorption Energy		Energy difference	
	hcp	bridge	ΔE(hcp−bridge)	ΔE(hcp−bridge)(ZPE)
PBE	−1.62	−1.58	−0.04 (hcp)	−0.01 (hcp)
PBE-D3(BJ)	−2.72	−2.70	−0.02 (hcp)	+0.01 (bridge)
PBE+vdW(TS)	−2.90	−2.92	+0.02 (bridge)	+0.04 (bridge)
vdW-DF2	−0.94	−0.85	−0.09 (hcp)	−0.07 (hcp)

Table 1 Calculated adsorption energies and energy differences (in eV) for benzene on Rh(111) at hcp0° and bridge30° sites using four different methods. The 5×5 unit cell was chosen to represent the isolated regime.

The four functionals used produce very different values for the lowest adsorption energy; PBE (-1.62 eV), PBE-D3(BJ) (-2.72 eV), PBE+vdW(TS) (-2.92 eV) and vdW-DF2 (-0.94 eV). Although the adsorption energy for benzene on Rh(111) has never been experimentally determined, it is expected to follow the trend determined by measurements on other 4d and 5d metals such as Pt(111)[11,48], thus the actual adsorption energy for benzene is expected to be somewhere around -2 eV or lower. The vdW-DF2 functional can therefore be dismissed as an unreliable method for these experiments, since the adsorption energies calculated are too high (-0.94 eV and -0.85 eV for hcp and bridge adsorption respectively) compared to the expected adsorption energy. This concurs with a recent study that found the vdW-DF and vdW-DF2 functionals to be

inaccurate in describing benzene adsorption in systems where strong chemisorption occurs. This same study also found the RPA method to provide the most accurate adsorption energies for benzene on various metals when compared to experimental values, while also predicting the adsorption energy at medium coverage of the Rh(111) surface to be 2.08 eV[72].

The relative energy difference between the two most stable adsorption sites are very similar for all functionals employed, with energy differences lower than 0.1 eV. The highest difference was found for the (inaccurate) vdW-DF2 functional (0.09 eV), with the lowest difference found for both the PBE-D3(BJ) and PBE+vdW(TS) methods (0.02 eV). Every functional employed except the PBE+vdW(TS) accurately predicts the most stable adsorption site of the two to be the hcp site, although the difference in the adsorption energy is low enough that it could possibly be considered within the error margins of the method. Even when ZPE corrections are applied, the energy difference remains low, with the only significant difference being that for the PBE-D3(BJ) functional, the most stable adsorption site switches from hcp for the uncorrected energies to bridge. The small energy differences reflect the experimental observations of benzene molecules in both adsorption sites (at low temperatures), with three of the four functionals accurately predicting that the hcp adsorption site is the most stable of the two. This suggests that that these functionals are sufficiently accurate to provide a qualitative understanding of the adsorption of benzene on Rh(111) at low coverage. Qualitatively speaking, applying ZPE corrections does not improve the accuracy of these results.

To examine the differences in the interaction of benzene with the Rh(111) substrate with respect to coverage, especially as it pertains to the potential adsorption sites and

ordering of the molecules, other experiments were performed where the Rh(111) surface was saturated with benzene. The next two sections of this paper will cover this part of our investigation.

B. The $(2\sqrt{3}\times3)$*rect* ordering of benzene at high coverage of the Rh(111) surface

The work presented in this section does not counter or contradict any of the prior publications where the deposition of benzene at high coverage on Rh(111) has been reported on, but the nature of this discussion will be relevant when we move on to investigate the (√19×√19)R23.4° ordering. In these previous experiments, mainly involving HREELS and LEED, benzene was found to form a short-ranged (2√3×3)*rect* ordered structure, with a unit cell containing two benzene molecules, each one adsorbed in a different bridge30° configuration[21,52,54]. Disordered molecules present on the surface were determined to be on three-fold hollow sites.

The existence of three possible bridge30° configurations for the benzene molecules suggests two possible arrangements for the (2√3×3)*rect* structure. When isolated, the molecules on these adsorption sites (labelled "α", "β" and "γ" in Figure 5a) are geometrically and energetically degenerate and are mirror images along the [11$\bar{2}$] direction of the substrate i.e. "α" converts into "β", while "γ" remains unchanged upon reflection. When the molecules arrange to form the (2√3×3)*rect* structure, the inter-adsorbate interactions within the unit cell result in the single molecule arrangements becoming non-degenerate. The two possible ways for the molecules to order are "bridge α + bridge β" and "bridge α + bridge γ" (since "bridge β + bridge α" and "bridge β + bridge γ" are symmetrically equivalent to "bridge α + bridge β" and "bridge α + bridge γ"

respectively) with the major difference between the two being that the unit cell for the latter configuration has no glide plane symmetry. The "bridge α + bridge β" and "bridge α + bridge γ" arrangements are shown in Figures 5b and 5c respectively. Previous research has observed the presence of glide plane symmetries through the extinction of specific spots in the (2√3×3)*rect* LEED pattern of benzene adsorbed on Rh(111)[52], thus the "bridge α + bridge β" ordering is expected while the "bridge α + bridge γ" structure is not. For comparison, another (2√3×3)*rect* arrangement is shown in Figure 5d, however the molecules are centered over the hollow sites instead of bridge sites.

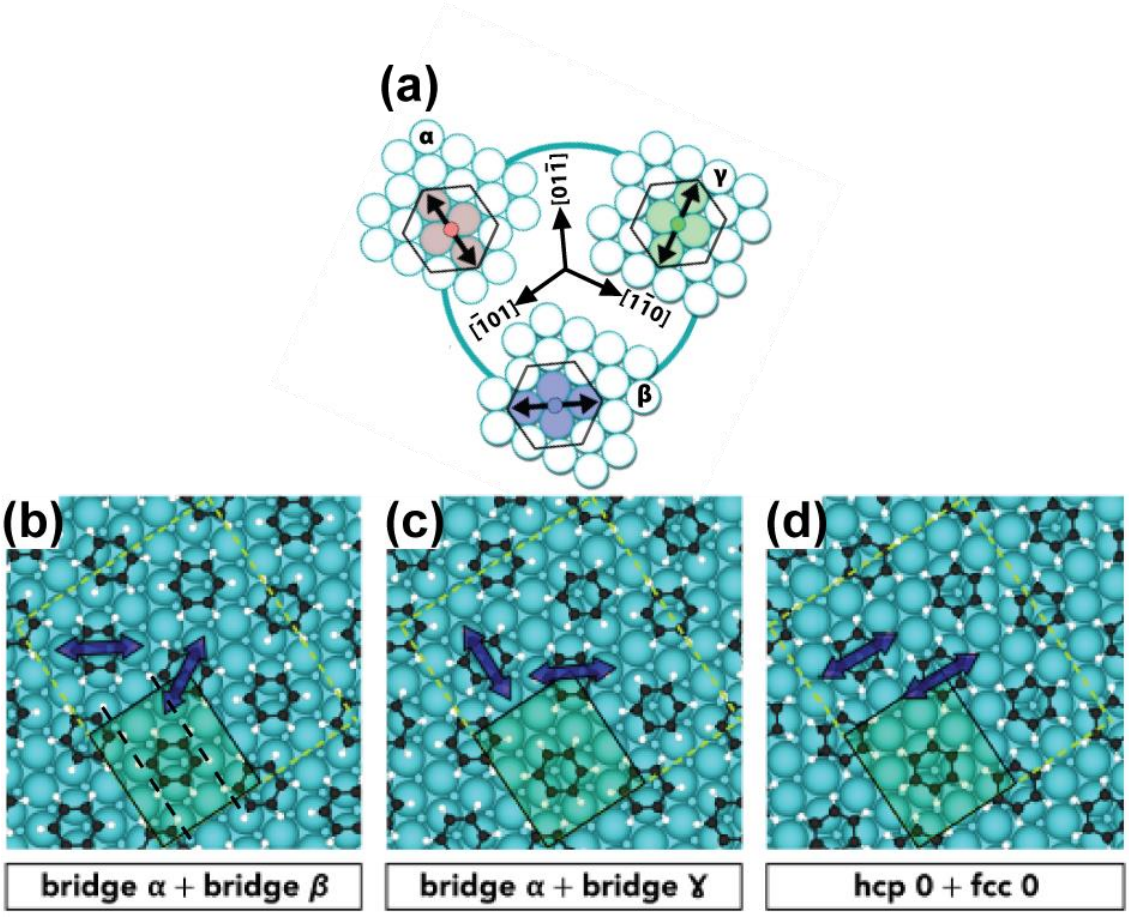

Figure 5(a) The three degenerate bridge30° configurations for benzene on Rh(111), labelled α (red), β (blue) and γ (green). Double headed arrows pointing to carbon atoms aligned in the [11$\bar{2}$] direction is used for reference. (b)-(d) Models of the optimized geometries for the three most theoretically stable (2√3×3)*rect* configurations of benzene

on Rh(111): (b) bridge α + bridge β, with black dashed lines used to indicate the location of the glide planes (c) bridge α + bridge γ and (d) hcp0° and fcc0°.

The direct observation of the Rh(111) surface through STM imaging after exposing the crystal to about 4 L of benzene at room temperature allows for the arrangement of the (2√3×3)*rect* structure to be confirmed, along with other observations made in prior investigations. For example, STM images like those in Figure 6 confirm the short coherence length of the (2√3×3)*rect* structure first suggested by LEED and HREELS analysis carried out by Mate *et al*[52]. The ordering is first identified in these images as the rectangular islands (some of which are highlighted in Figure 6), with the size of the unit cell and the distance between the nearest neighbor benzene molecules used to confirm their identity. Alongside the short-ranged ordered domains are clusters consisting of a few molecules, which resemble extremely localized (2√3×3)*rect* structures. This ordering must be induced by the increased packing of the surface with benzene, meaning the repulsive interaction between the molecules is compensated for by the attractive interaction between the benzene and the surface atoms (i.e. the adsorption energy) at high coverages. Therefore, the arrangement of the molecules into a dense (2√3×3)*rect* structure appears to lead to a minimization of the total energy across the surface.

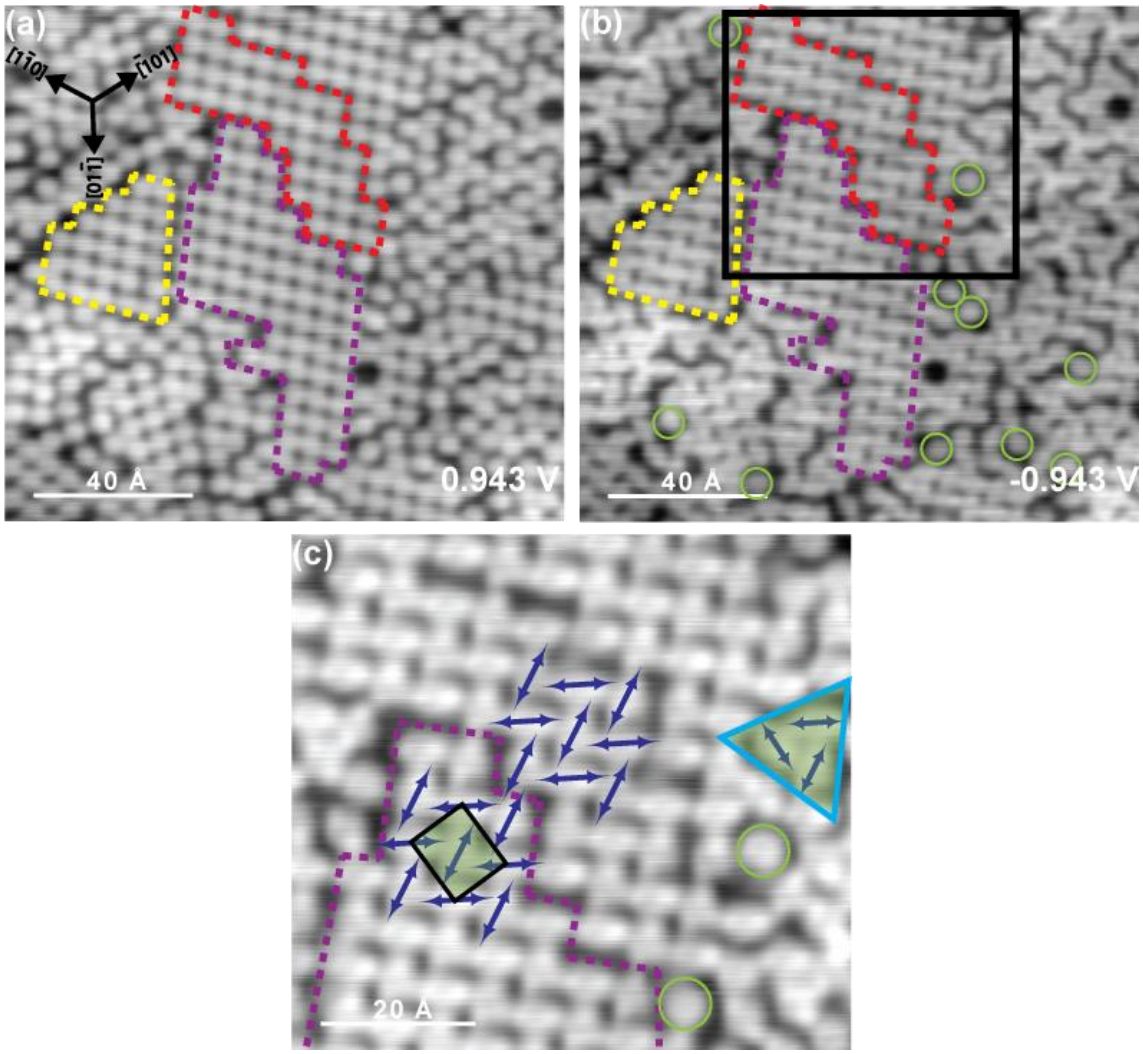

Figure 6(a) and (b) 140×140 Å^2 constant current images (I_t= 0.099 nA) of benzene on Rh(111), deposited at room temperature at saturation coverage. Three different domains of (2√3×3)*rect* are highlighted by dashed lines (yellow, red and purple). Image (a) was acquired with a bias of 0.943 V, while image (b) was acquired with a bias of -0.943 V. The molecules circled in green in (b) are ones that have not changed in appearance upon changing the polarity of the bias and thus are expected to be adsorbed on hollow sites. (c) 72×72 Å^2 constant current image (I_t= 0.25 nA, V= -0.943 V) taken over the area highlighted by the black square shown in (b). Double sided arrows are used to indicate the elongation axis of the molecules, emphasizing the two orientations of benzene in the (2√3×3)*rect* unit cell (green rectangle), as well as the three orientations of benzene in the isolated clusters of three molecules (green triangle).

Scanning at negative bias in constant current mode (note that in this experimental setup it is the sample that is biased) allows for the clarification of the adsorption sites for the benzene molecules, even without high resolution, as shown in Figure 6. While

the molecules have a near identical electronic contrast when scanned at positive bias (appearing as round protrusions in Figure 6a), in Figure 6b (acquired at negative bias over the same scan area) most of the features take on a distorted appearance reminiscent of the bridge site adsorbed benzene molecule identified at low coverage in Figure 3, including those molecules that are part of the (2√3×3)*rect* domains. This is most obvious in the high magnification image shown in Figure 6c. Within a unit cell of the (2√3×3)*rect* ordering (highlighted in the STM image in Figure 6c by the green rectangle), the axis of elongation for the two molecules are rotated by 60° with respect to one another, thereby confirming that the two benzene molecules are adsorbed onto alternating bridge sites.

The switch in polarity between the images in Figures 6a and 6b also provides insight into the adsorption behavior of those molecules not part of the (2√3×3)*rect* ordering. Many of the disordered molecules are also observed to be on bridge sites, as they also take on the distorted appearance associated with bridge site adsorption at negative polarity. They also appear to cluster together, mainly in a triangular arrangement comprised of three benzenes, one of which is highlighted by a green triangle in Figure 6c. Another noticeable cluster consists of five benzene molecules which resembles two of the smaller triangular arrangements sharing a common benzene. Within this triangular cluster, the axis of elongation for the three molecules are all rotated by 60° with respect to one another, thus all three benzenes are adsorbed onto a different bridge site. This structure is significant in the discussion of the (√19×√19)R23.4° ordering in the next section of this paper. There are also a few molecules, highlighted by green circles in Figure 6b, that remain unchanged from their appearance as round protrusions

in Figure 6a. These molecules are determined to be the ones adsorbed on three-fold hollow sites as previously identified by HREELS experiments[41]. Statistical analysis of STM images like those in Figure 6 reveals that less than ten percent of the benzene molecules at this coverage are in three-fold hollow sites.

High resolution images acquired in constant height mode are required to elucidate the specific bridge site the molecule is adsorbed onto using a model of the first layer of the Rh(111) substrate. By making the model appropriately to scale with a given image, the molecules in the image cannot be forced onto incorrect adsorption sites. An example of this is shown in Figure 7, which confirms that the expected "bridge α + bridge β" arrangement (where the molecules alternate between two different bridge30° configurations) is observed for the (2√3×3)*rect* structure due to the presence of glide plane symmetry within the ordering. The locations of the glide planes are identified by the white dashed lines passing through the (2√3×3)*rect* unit cell shown in Figure 7.

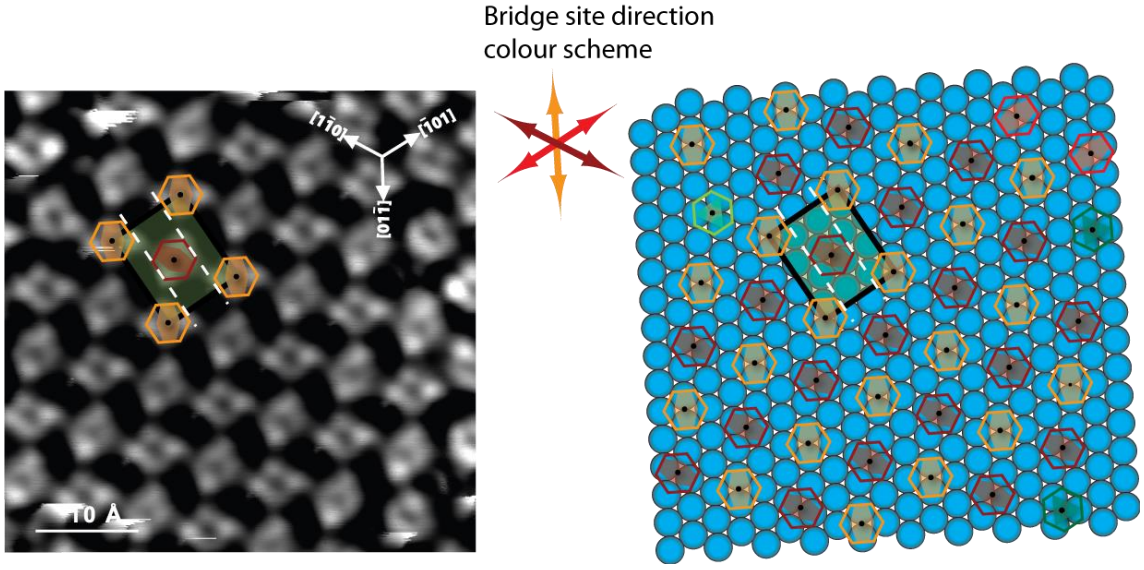

Figure 7 Left: 46×47 Å^2 constant height image (V= 50 mV) of benzene saturated on Rh(111), with most of the molecules in the (2√3×3)*rect* arrangement. The rectangular unit cell for this ordering is shown on the image, with the white dashed lines indicating the location of the glide planes. Right: Model of benzene on Rh(111) from the

image on the left. The dark red, red and orange molecules are adsorbed onto different bridge sites, with the green molecules adsorbed on hollow sites (dark green for hcp, light green for fcc).

The analysis of high resolution images like those in Figure 7 provides information regarding the relationship between the electronic contrast of the benzene molecules with respect to the precise bridge site it is adsorbed onto. Specifically, the elongation of the molecule occurs along the axis perpendicular to the bridge site orientation with respect to the high symmetry direction of the substrate. The brighter contrast observed at either stretched end is a consequence of having a carbon atom positioned almost directly above a rhodium atom in the surface (these observations also hold for the benzene observed on an isolated bridge site at low coverage in Figure 3). A few of the molecules in this image do not take on the same distorted appearance as those on bridge sites; these are confirmed by the model to be adsorbed onto hollow sites. Perhaps somewhat surprisingly, the model also reveals the existence of benzene molecules on both types of three-fold hollow sites (knowledge of the second layer has allowed us to determine that two of the molecules, represented by the dark green hexagons in Figure 7, are adsorbed on a hcp site, with the third, represented by a light green hexagon in Figure 7, on an fcc site). It stands to reason that the dense packing of the surface, already responsible for the rearrangement of the molecules into the (2√3×3)*rect* ordered islands, allows for the adsorption of benzene in this otherwise unfavorable position (as determined by our own theoretical investigations as well as previously published work[39,44,70,71] although admittedly none of these results are based on models of benzene adsorption where the intermolecular distance is at such a short range as seen in these experiments).

Theoretical studies were employed here to better investigate the adsorption arrangement of the benzene molecules within the (2√3×3)*rect* structure, since we need to understand why the structure does not absorb in any other arrangement despite the existence of three bridge30° configurations for benzene to adsorb onto. The adsorption energy for benzene in this ordering was calculated using four different functionals, alongside the other arrangements shown in Figure 5 (which are not experimentally observed), with the results displayed in Table 2. The "bridge α + bridge γ" arrangement is the only other way the molecules can be adsorbed onto alternating bridge sites, while the "hcp0° + fcc0°" is the only other feasible arrangement where the molecules are adsorbed onto two different bridge sites within the unit cell. Previous investigations have shown that the other possible configurations for benzene adsorption (including top sites with any orientation and the hollow sites oriented 0° with respect to the surface) would be too unstable to occur, either in isolation or as part of a dense ordering[71].

Methods	Adsorption Energy		
	bridge α + bridge β	bridge α + bridge γ	hcp 0 + fcc 0
PBE	−2.43	−1.60	−1.90
PBE-D3(BJ)	−4.95	−4.07	−4.30
PBE+vdW(TS)	−5.36	−4.46	−4.58
vdW-DF2	−1.27	α+β	−0.95

Table 2 Calculated adsorption energies (in eV) for benzene on Rh(111) in the (2√3×3)*rect* arrangement for the three configurations shown in Figure 6. Note that for vdW-DF2, the α+γ configuration converts to α+β during optimization.

All methods accurately predict the experimentally observed "α and β" configuration as the most stable. The difference in energy with the other structures is significant, with the least stable structure, the "α and γ" structure, at least 0.83 eV higher in adsorption energy than the "α and β" structure, while the "hcp and fcc" structure is between 0.32 and 0.78 eV less stable, depending on the method used. The significant energetic differences are attributed to the repulsive interaction between the molecules; the symmetric positioning of the benzenes in the "α and β" arrangement allows for the minimum interaction possible between molecules within such a dense structure. Neither of the other two arrangements have glide plane symmetry, resulting in the distance between nearest neighbor molecules being smaller than in the "α and β" arrangement. The strength of the repulsion follows on from the trend established in the earlier discussion about the low coverage experiments, where a significant increase in adsorption energy was observed for all methods going from a (5×5) unit cell to a (3×3) unit cell.

C. The $(\sqrt{19}\times\sqrt{19})$R23.4° ordering of benzene

The only difference in the preparation of the dense (√19×√19)R23.4° ordering of benzene on Rh(111) and the (2√3x3)*rect* structure is the annealing of the crystal to 363 K, either during or after the deposit of a high coverage (≥1 L) of benzene. When this arrangement of the benzene molecules was first identified through LEED and ARUPS measurements by Neuber *et al*[31], the unit cell was hypothesized to be comprised of three benzene molecules adsorbed onto the three different bridge sites (as opposed to two bridge sites for the (2√3×3)*rect* unit cell), although the exact adsorption sites were not determined. As the (√19×√19)R23.4° and the (2√3×3)*rect* ordering are both similarly

dense (the latter has six rhodium atoms per benzene molecule, while the former is less dense with 6.33 atoms per benzene), the same rules govern the precise arrangement of the molecules in both structures. The distribution of benzene within the ordering must result in a minimization of the steric hindrance between the hydrogens of the nearest neighbor molecules. If we simply consider the molecules to adsorb onto the bridge sites (in the bridge30° configuration), then there are four possible ways the molecules can arrange themselves to form the (√19×√19)R23.4° ordering, as shown in Figure 8.

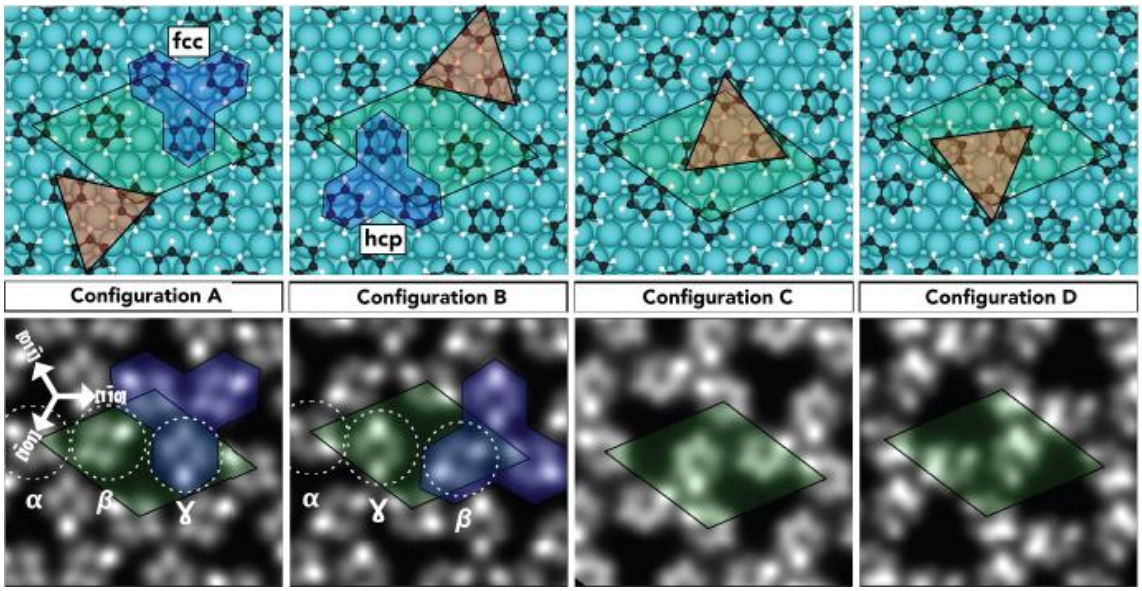

Figure 8 Models of the optimized geometries for the four possible configurations of the (√19×√19)R23.4° ordering of benzene on Rh(111). The corresponding simulated STM images are shown below each configuration. The green rhombi highlight the (√19×√19)R23.4° unit cell in each case, while the propeller shaped polygon in blue highlights the difference between configuration A and B; in A, the propeller is centered over an fcc site, while in B it is centered over a hcp site. The red triangles are used to highlight the orientation of the triangular clusters first observed in Figure 6 during the discussion of the (2√3x3)*rect* ordering

Each configuration is comprised of the triangular clusters that were first identified amongst the (2√3x3)*rect* ordering, as imaged in Figure 6. The molecules in these clusters are arranged in such a way that they go from the "α" to "β" to "γ" (using the same

notation established in Figure 5) orientations in a clockwise direction. Configuration A and B in Figure 8 are geometrically equivalent with respect to the top layer of the surface (i.e. they are the mirror image of one another through the $[1\bar{1}0]$ plane), however they are not energetically equivalent to one another, since the reflection through the mirror plane results in the exchange of hollow site positions. To help visualize this, a propeller shaped visual aid is highlighted in blue in Figure 8 in the images/models of the two configurations; the center of the propeller is at a three-fold hollow site, specifically an fcc site for configuration A and an hcp site for configuration B. The same difference is also observed when comparing configurations C and D.

The STM images presented in Figure 9 are the first direct observation of the (√19×√19)R23.4° ordering, during which only one configuration was observed. The domain of ordering shown in Figure 9a is one of the larger islands observed during this investigation, as domains of shorter coherence length were found to be more prominent. A few domains of (2√3×3)*rect* ordering were also identified during these measurements, but nothing larger than the domain observed in Figure 9b and there was significantly more (√19×√19)R23.4° ordering. The coexistence of these structures and the conditions under which they form will be discussed later in this paper.

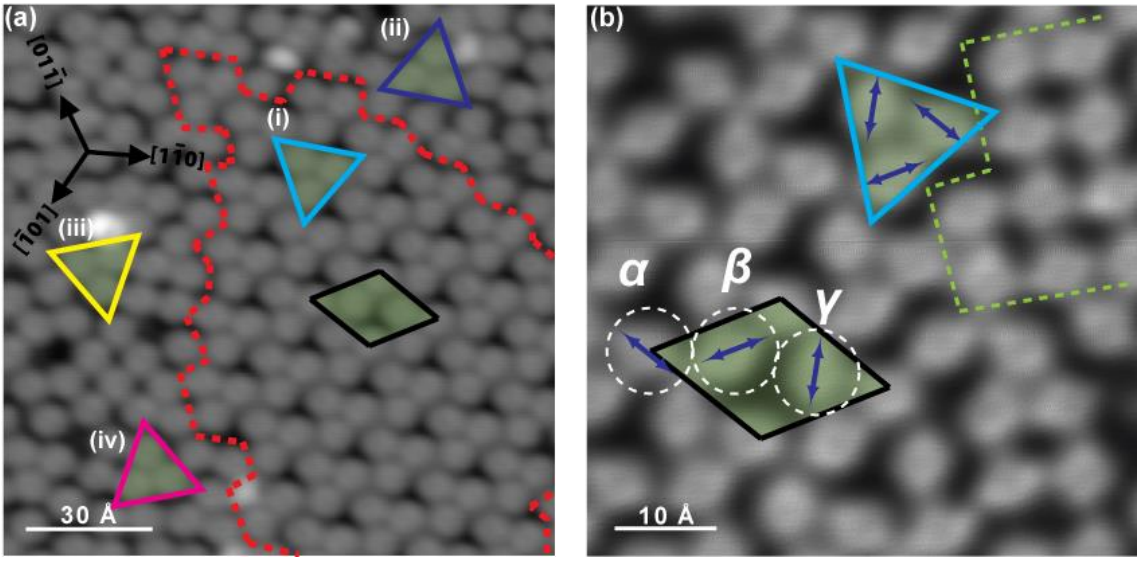

Figure 9(a) 108×108 Å^2 constant current image (I_t= 0.11 nA, V= 0.927 V) of benzene on Rh(111) at saturation coverage. The substrate was annealed to 363 K after the molecular deposition, resulting in the formation of the (√19×√19)R23.4° structure, a domain of which is highlighted by the dotted red lines in this image. The primitive unit cell for the (√19×√19)R23.4° structure is also highlighted in this image. The ordering is comprised of clusters of three benzene molecules, highlighted by triangle (i), while three isolated clusters are identified with a different orientation at (ii)-(iv). (b) 54×52 Å^2 constant height image (V= 93 mV). Double headed arrows are used to indicate the axis of elongation in the image for each molecule in the unit cell of the (√19×√19)R23.4° structure and the cluster of three benzene molecules. A (2√3×3)*rect* domain is highlighted by the green dashed line.

Once again, the electronic contrast for benzene displays the two-fold elongation associated with the molecules adsorption on bridge sites, with the three molecules in the unit cell on a geometrically different bridge site. This is evident from the fact that the elongated features are rotated by 60° with respect to one another. These images make it simple to identify the triangular clusters that can be considered to be the "building blocks" of the (√19×√19)R23.4° structure, with an example of one highlighted by the blue triangle in Figure 9. These clusters also continue to exist on the surface after depositing at 363 K in an isolated form i.e. they are not part of the larger (√19×√19)R23.4° ordering, making them the most dominant feature present in the STM images. The existence of these clusters at room temperature, along with the coexistence

of the (√19×√19)R23.4° and (2√3×3)*rect* ordering in these experiments, indicates that the energy required to form both of these structures is relatively similar.

Although all four possible orientations of the triangular clusters are observed in Figure 9a isolated from any domains of ordering, as highlighted by triangles (i)-(iv), only one configuration is observed for the (√19×√19)R23.4° structure. Based on our STM images, this configuration is either A or B from Figure 8. To distinguish between these two configurations, a triangular vacancy defect was once again imaged during the course of these STM measurements, allowing for the identification of the location of the hollow sites in the top layer of the substrate (using the same method used in the analysis of benzene adsorption in the low coverage regime above). Therefore, configuration A from Figure 8 was experimentally determined to be the correct arrangement for the benzene molecules in the (√19×√19)R23.4° ordering.

Calculating the adsorption energies for benzene for configurations A-D allow for a better understanding as to why A is the only one observed to form, despite the existence of the triangular cluster "building blocks" for the other three arrangements. The results of these calculations are presented in Table 3, which confirms that configuration A is the most stable structure, regardless of the functional used. Configuration B was found to be only 10-30 meV less stable, which is unsurprising as they only differ in the position of the molecules with respect to the second layer of the substrate, as discussed earlier. Even the interlacing of the hydrogen atoms on neighboring benzene molecules is the same. The other configurations, C and D, are significantly less stable than either A and B; even the lowest difference in energy compared with configuration A, found using the vdW-DF2 functional, was 0.30 and 0.37 eV for configurations C and D respectively.

Methods	Adsorption Energy			
	Configuration A	Configuration B	Configuration C	Configuration D
PBE	−3.84	−3.82	−3.32	−3.26
PBE-D3(BJ)	−7.53	−7.50	−7.00	−6.94
PBE+vdW(TS)	−8.22	−8.19	−7.60	−7.52
vdW-DF2	−1.94	−1.93	−1.63	−1.56

Table 3 Calculated adsorption energies (in eV) for benzene on Rh(111) in the (√19×√19)R23.4° arrangement for the four configurations shown in Figure 8.

The difference between configurations C and D compared to A and B are highlighted by an event that occurred during the modelling of these structures. When C and D were modelled for the calculation of the adsorption energy of benzene in the (√19×√19)R23.4° ordering, the molecules were forced to rotate slightly off their bridge30° site. This explains the topography of the simulated STM images for configurations C and D shown in Figure 8, with the molecules no longer possessing the two-fold symmetry expected for benzene imaged on bridge sites, instead appearing even more distorted. Neuber *et al*[31] proposed a similar arrangement to configuration A when they identified the (√19×√19)R23.4° ordering for the first time, but also placed the molecules slightly off the bridge30° sites, presumably to limit steric hindrance. Since the experimental images of this structure match the simulated STM images for configuration A, the molecules can be confirmed to be precisely on bridge30° sites.

More theoretical investigations were necessary to understand the differences in the driving force behind the two dense ordered benzene structures. Table 4 reveals the results for the computed adsorption energies per benzene molecule and per unit area for both dense structures as well as the low coverage regime (modelled with the 5×5

unit cell first used in Figure 3 and Table 1). These calculations were performed mainly due to the observation the coexistence of the two dense benzene structures after depositing with the substrate at 363 K, while only the (2√3×3)*rect* is observed after depositing at room temperature. Since the structures differ in terms of the number of benzene molecules per unit cell, then calculating the adsorption energy for benzene in each arrangement could provide insight into these experimental observations. The low coverage regime is also considered for comparison with these dense structures. For the energy per molecule, the low coverage regime is unsurprisingly thermodynamically more stable than either of the dense structures, due to the strong repulsive interaction between the benzene molecules. As such, the energy per molecule for the low coverage is between 0.18 and 0.38 eV lower in energy than the dense structures. In contrast, there is only a slight difference in the energy between the two dense ordered structures. Unsurprisingly, a lower adsorption energy per molecule is observed with the (√19×√19)R23.4° ordering as opposed to the (2√3×3)*rect* structure. This result will stem from the fact that the (2√3×3)*rect* ordering is slightly denser, with 6.33 rhodium atoms per benzene molecule compared to six atoms per molecule within the (√19×√19)R23.4° structure.

Methods	Adsorption Energy per molecule		
	Low coverage	$(2\sqrt{3}\times3)rect$	$(\sqrt{19}\times\sqrt{19})$R23.4°
PBE	−1.59	−1.22	−1.28
PBE-D3(BJ)	−2.69	−2.48	−2.51
PBE+vdW(TS)	−2.92	−2.68	−2.74
vdW-DF2	−0.94	−0.63	−0.65
	Adsorption Energy per unit area		
PBE	−0.10	−0.32	−0.32
PBE-D3(BJ)	−0.17	−0.66	−0.64
PBE+vdW(TS)	−0.19	−0.72	−0.70
vdW-DF2	−0.06	−0.16	−0.15

Table 4 Summary of the calculated adsorption energies for pure benzene on Rh(111) for the different structures observed in this study. This includes the adsorption energy per molecule (in eV/molecule) and the adsorption energy per unit area (in eV nm^{-2}). The isolated, low coverage regime was modelled using a 5×5 unit cell.

For the ordered structures to be able to form, the energy penalty incurred by the repulsive inter-adsorbate interaction must be compensated for by the gain in energy achieved by the surface adsorbing more molecules per unit area. This is reflected by the changing trends observed in Table 4 when we compare the calculated results for the adsorption energy per molecule and per unit area. Independent of the method used, a significant gain in energy per unit area is achieved upon going from the low coverage regime to the two dense structures. This gain in energy is why the formation of these structures are favored and is thus the driving force behind the organization of benzene at high coverage.

Although three of the four functionals used favor the (2√3×3)*rect* ordering over the (√19×√19)R23.4° ordering when examining the adsorption energy per unit area, the differences in energy are no higher than 20 meV per nm^2 of surface covered. This

correlates with the experimental observations of both structures simultaneously upon saturating the surface with benzene molecules at 363 K and also provides an explanation as to why the "building blocks" for the (√19×√19)R23.4° structure, the triangular clusters comprised of three benzenes, are observed in isolation from the ordered structure, no matter the temperature of the substrate during or after the deposition. However, the results shown in Table 4 do not adequately explain why only the (2√3x3)*rect* structure is observed after depositing at room temperature. The formation of the (√19x√19)R23.4° ordering can only be achieved by increasing the temperature of the substrate to 363 K either during or after the molecular deposition onto the Rh(111) surface. Therefore, we propose that an energy barrier exists at lower temperatures which hinders the formation of the (√19×√19)R23.4° arrangement of benzene molecules. Only thermal energy is required to overcome the barrier, after which both dense structures can coexist (up until benzene decomposition occurs at approximately 413 K[50]), as observed in our STM measurements, due to the similarity in adsorption energy between the two structures. The mechanism for the formation of the (√19×√19)R23.4° structure is also proposed to be the rearrangement of molecules from the (2√3x3)*rect* ordering as evident from the decrease in the size of the domains of the rectangular structure.

Conclusion

In summary, this study provided a thorough investigation into the chemisorption of pure benzene on Rh(111) using a combination of STM imaging and DFT calculations. The focus was given to characterizing the benzene/Rh(111) system at two different coverages; low coverage (which had previously not been investigated) and high coverage. Analysis of the STM images revealed isolated, disordered molecules that were not even prone to molecular pairing, with the molecules determined to be adsorbed on

hcp0° sites. Four different functionals were used for all DFT calculations performed throughout this investigation and when used to model the low coverage regime, revealed an energy penalty was incurred by bringing the molecules closer together, proving the existence of a strong inter-adsorbate repulsive interaction between the benzene molecules. Most of the functionals also accurately determined the hcp0° adsorption of benzene, with only a small difference in energy observed between hcp0° adsorption and bridge30° adsorption. This explains the observation of benzene in bridge30° sites as a minor species present after depositing at around 150 K.

At high coverage, the first direct observation of the (√19×√19)R23.4° structure was accomplished via STM. This structure coexists with the slightly denser (2√3×3)*rect* ordering, although only if the substrate has been annealed to 363 K either during or after the deposition process. Only the (2√3×3)*rect* ordering exists after depositing at room temperature. In either case, disordered molecules exist as well, although most of these molecules are clustered together in groups of three. Within these clusters, the benzene molecules can be visually identified to be adsorbed onto bridge sites, with each molecule identified to be on a different type of bridge site. These clusters can be described as the "building blocks" for both of these dense structures.

The driving force behind the arrangement of benzene molecules at high coverage can also be explained. Upon calculating the adsorption energy per unit area for benzene at low coverage and in the two dense structures, the energy is significantly lower for the dense ordering, thus the structures are thermodynamically driven to form, overcoming the repulsion between the individual molecules. The energy gain however is not enough to allow for the formation of islands with a large coherence length, as observed

experimentally. The adsorption energy per unit area is very similar for both ordered structures for all functionals applied, despite the experimental observation of the (√19×√19)R23.4° overlayer exclusively forming at 363 K and not at lower temperatures, unlike the (2√3×3)*rect* ordering which forms at room temperature and at 363 K. It is therefore proposed that an activation barrier exists for the formation of the (√19×√19)R23.4° structure that can be overcome by increasing the temperature of the substrate. Overcoming this barrier results in the rearrangement of some of the molecules in the (2√3×3)*rect* domains in order to form the new, slightly less dense structure.

Acknowledgements

We acknowledge financial support from the Scottish Funding Council (through EaStCHEM and SRD-Grant HR07003) and from EPSRC (PhD studentships for JAGT – EP/M506631/1, and MJT – EP/K503162/1). Computational support was provided via the EaStCHEM Research Computing Facility.

Author contributions

RS conceived and designed the study. MJT and CJB prepared samples, acquired and analyzed STM data. JAGT conducted and analyzed DFT calculations. All of the authors discussed the experimental and theoretical results. All of the authors contributed to the interpretation of the data. MJT and RS wrote the manuscript.

References

(1) Netzer, F. P.; Bertel, E.; Matthew, J. A. D. Sensitivity of Electronic Transitions to Molecule-Surface Orientation: ELS of Benzene and Pyridene on Ir(111). *Surf. Sci.* **1980**, *92*, 43–52.

(2) Richardson, N. V.; Palmer, N. R. A Comparison of Chlorobenzene and Benzene Adsorption on Pt{001}. *Surf. Sci.* **1982**, *114*, L1–L6.

(3) Lauhon, L. J.; Ho, W. Single-Molecule Chemistry and Vibrational Spectroscopy: Pyridine and Benzene on Cu(001). *J. Phys. Chem.* **2000**, *104*, 2463–2467.

(4) Morin, C.; Simon, D.; Sautet, P. Chemisorption of Benzene on Pt(111), Pd(111), and Rh(111) Metal Surfaces : A Structural and Vibrational Comparison from First Principles. *J. Phys. Chem. B* **2004**, *108*, 5653–5665.

(5) Liu, G.-K.; Ren, B.; Wu, D.-Y.; Duan, S.; Li, J.-F.; Yao, J.-L.; Gu, R.-A.; Tian, Z.-Q. Effect of Intrinsic Properties of Metals on the Adsorption Behavior of Molecules: Benzene Adsorption on Pt Group Metals. *J. Phys. Chem. B* **2006**, *110*, 17498–17506.

(6) Netzer, F. P.; Mack, J. U. The Electronic Structure of Aromatic Molecules Adsorbed on Pd(111). *J. Chem. Phys.* **1983**, *79*, 1017–1025.

(7) Waddill, G. D.; Kesmodel, L. L. Benzene Chemisorption on Palladium Surfaces. I. High-Resolution Electron-Energy-Loss Vibrational Spectra and Structural Models. *Phys. Rev. B* **1985**, *31*, 4940–4946.

(8) Netzer, F. P.; Rangelov, G.; Rosina, G.; Saalfeld, H. B.; Neumann, M.; Lloyd, D. R.

Benzene on Pd(110): The First Example of Nonparallel Adsorption. *Phys. Rev. B* **1988**, *37*, 10399–10402.

(9) Ohtani, H.; Van Hove, M. A.; Somorjai, G. A. Molecular Structure of Benzene Coadsorbed with CO on Pd(111): A Dynamical Low-Energy Electron Diffraction Analysis. *J. Phys. Chem.* **1988**, *92*, 3974–3982.

(10) Dudde, R.; Frank, K. H.; Koch, E. E. The Electronic Structure of Benzene Adsorbed on Ag(111) Studied by Angle Resolved Photoemission. *Surf. Sci.* **1990**, *225*, 267–272.

(11) Wander, A.; Held, G.; Hwang, R. Q.; Blackman, G. S.; Xu, M. L.; de Andres, P.; Van Hove, M. A.; Somorjai, G. A. A Diffuse LEED Study of the Adsorption Structure of Disordered Benzene on Pt(111). *Surf. Sci.* **1991**, *249*, 21–34.

(12) Weiss, P.; Eigler, D. Site Dependence of the Apparent Shape of a Molecule in Scanning Tunneling Micoscope Images: Benzene on Pt{111}. *Phys. Rev. Lett.* **1993**, *71*, 3139–3142.

(13) Xi, M.; Yang, M. X.; Jo, S. K.; Bent, B. E.; Stevens, P. Benzene Adsorption on Cu(111): Formation of a Stable Bilayer. *J. Chem. Phys.* **1994**, *101*, 9122–9131.

(14) Somorjai, G. A. *Chemistry in Two Dimensions: Surfaces*; Cornell University Press: New York, 1981.

(15) Stanislaus, A.; Cooper, B. H. Aromatic Hydrogenation Catalysis: A Review. *Catal. Rev.* **1994**, *36*, 75–123.

(16) Fu, X. Z.; Zeltner, W. A.; Anderson, M. A. The Gas-Phase Photocatalytic

Mineralization of Benzene on Porous Titania-Based Catalysts. *Appl. Catal. B-Environmental* **1995**, *6*, 209–224.

(17) Cooper, B. H.; Donnis, B. B. L. Aromatic Saturation of Distillates: An Overview. *Appl. Catal. A Gen.* **1996**, *137*, 203–223.

(18) Dahlberg, S. C.; Musser, M. E. The Surface Photovoltage of an Increasing Series of Polyarenes: Anthracene, Tetracene, and Pentacene. *J. Chem. Phys.* **1979**, *71*, 2806–2810.

(19) Würthner, F. Plastic Transistors Reach Maturity for Mass Applications in Microelectronics. *Angew. Chemie - Int. Ed.* **2001**, *40*, 1037–1039.

(20) Picciolo, L. C.; Murata, H.; Kafafi, Z. H. Organic Light-Emitting Devices with Saturated Red Emission Using 6,13-Diphenylpentacene. *Appl. Phys. Lett.* **2001**, *78*, 2378–2380.

(21) Koel, B. E.; Crowell, J. E.; Mate, C. M.; Somorjai, G. A. A High-Resolution Electron Energy Loss Spectroscopy Study of the Surface Structure of Benzene Adsorbed on the Rhodium(111) Crystal Face. *J. Phys. Chem.* **1984**, *88*, 1988–1996.

(22) Neumann, M.; Mack, J. U.; Bertel, E.; Netzer, F. P. The Molecular Structure of Benzene on Rh(111). *Surf. Sci.* **1985**, *155*, 629–638.

(23) Bertel, E.; Rosina, G.; Netzer, F. P. The Structure of Benzene on Rh(111): Coadsorption with CO. *Surf. Sci. Lett.* **1986**, *172*, L515–L522.

(24) Netzer, F. P. Surface Structure and Reactivity of Aromatic Molecules: Can We Track Down Trends in the Periodic Table? *Langmuir* **1991**, *7*, 2544–2547.

(25) Somorjai, G. A. *Introduction to Surface Chemistry and Catalysis*; John Wiley: New York, 1994.

(26) Triguero, L.; Pettersson, L. G. M.; Minaev, B.; Ågren, H. Spin Uncoupling in Surface Chemisorption of Unsaturated Hydrocarbons. *J. Chem. Phys.* **1998**, *108*, 1193–1205.

(27) Bilić, A.; Reimers, J. R.; Hush, N. S.; Hoft, R. C.; Ford, M. J. Adsorption of Benzene on Copper, Silver, and Gold Surfaces. *J. Chem. Theory Comput.* **2006**, *2*, 1093–1105.

(28) Lehwald, S.; Ibach, H.; Demuth, J. Vibration Spectroscopy of Benzene Adsorbed on Pt(111) and Ni(111). *Surf. Sci.* **1978**, *78*, 577–590.

(29) Van Hove, M. A.; Lin, R. F.; Somorjai, G. A. Surface Structure of Coadsorbed Benzene and Carbon Monoxide on the Rhodium(111) Single Crystal Analyzed with Low-Energy Electron Diffraction Intensities. *J. Am. Chem. Soc.* **1986**, *108*, 2532–2537.

(30) Koel, B. E.; Crowell, J. E.; Bent, B. E.; Mate, C. M.; Somorjai, G. A. Thermal Decomposition of Benzene on the Rh(111) Crystal Surface. *J. Phys. Chem.* **1986**, *90*, 2949–2956.

(31) Neuber, M.; Schneider, F.; Zubrägel, C.; Neumann, M. A Dense and CO Free Benzene Structure on Rh (111). *J. Phys. Chem.* **1995**, *99*, 9160–9168.

(32) Lee, A. F.; Wilson, K.; Lambert, R. M.; Goldoni, A.; Baraldi, A.; Paolucci, G. On the Coverage-Dependent Adsorption Geometry of Benzene Adsorbed on Pd{111}: A

Study by Fast XPS and NEXAFS. *J. Phys. Chem. B* **2000**, *104*, 11729–11733.

(33) Liu, W.; Maaß, F.; Willenbockel, M.; Bronner, C.; Schulze, M.; Soubatch, S.; Tautz, F. S.; Tegeder, P.; Tkatchenko, A. Quantitative Prediction of Molecular Adsorption: Structure and Binding of Benzene on Coinage Metals. *Phys. Rev. Lett.* **2015**, *115*, 036104.

(34) Bertolini, J. C.; Dalmai-Imelik, G.; Rousseau, J. Benzene Adsorption on Nickel (100) and (111) Faces Studied by Leed and High Resolution Electron Energy Loss Spectroscopy. *Surf. Sci.* **1977**, *67*, 478–479.

(35) Witte, G.; Range, H.; Toennies, J.; Wöll, C. Observation of the Low-Energy External Vibrations of Benzene on Rh(111). *Phys. Rev. Lett.* **1993**, *71*, 1063–1066.

(36) Yau, S.-L.; Kim, Y.-G.; Itaya, K. In Situ Scanning Tunneling Microscopy of Benzene Adsorbed on Rh (111) and Pt (111) in HF Solution. *J. Am. Chem. Soc.* **1996**, *118*, 7795–7803.

(37) Yoon, H. A.; Salmeron, M.; Somorjai, G. A. Scanning Tunneling Microscopy (STM) Study of Benzene and Its Coadsorption with Carbon Monoxide on Rh(111). *Surf. Sci.* **1997**, *373*, 300–306.

(38) Canduela-Rodriguez, G.; Sabbe, M. K.; Reyniers, M. F.; Joly, J. F.; Marin, G. B. Periodic DFT Study of Benzene Adsorption on Pd(100) and Pd(110) at Medium and Saturation Coverage. *J. Phys. Chem. C* **2014**, *118*, 21483–21499.

(39) Carrasco, J.; Liu, W.; Michaelides, A.; Tkatchenko, A. Insight into the Description

of van Der Waals Forces for Benzene Adsorption on Transition Metal (111) Surfaces. *J. Chem. Phys.* **2014**, *140*, 084704.

(40) Lakshmikanth, K. G.; Ayishabi, P. K.; Chatanathodi, R. Ab Initio DFT Studies of Adsorption Characteristics of Benzene on Close-Packed Surfaces of Transition Metals. *Comput. Mater. Sci.* **2017**, *137*, 10–19.

(41) Ayishabi, P. K.; Lakshmikanth, K. G.; Chatanathodi, R. Chemisorption of Benzene on Pt (111) Surface: A DFT Study with van Der Waals Interaction. *Chem. Phys. Lett.* **2015**, *637*, 182–188.

(42) Tonigold, K.; Groß, A. Adsorption of Small Aromatic Molecules on the (111) Surfaces of Noble Metals: A Density Functional Theory Study with Semiempirical Corrections for Dispersion Effects. *J. Chem. Phys.* **2010**, *132*, 224701.

(43) Ruiz, V. G.; Liu, W.; Zojer, E.; Scheffler, M.; Tkatchenko, A. Density-Functional Theory with Screened van Der Waals Interactions for the Modeling of Hybrid Inorganic-Organic Systems. *Phys. Rev. Lett.* **2012**, *108*, 146103.

(44) Liu, W.; Carrasco, J.; Santra, B.; Michaelides, A.; Scheffler, M.; Tkatchenko, A. Benzene Adsorbed on Metals: Concerted Effect of Covalency and van Der Waals Bonding. *Phys. Rev. B* **2012**, *86*, 245405.

(45) Morin, C.; Simon, D.; Sautet, P. Trends in the Chemisorption of Aromatic Molecules on a Pt(111) Surface: Benzene, Naphthalene, and Anthracene from First Principles Calculations. *J. Phys. Chem. B* **2004**, *108*, 12084–12091.

(46) Schaff, O.; Fernandez, V.; Hofmann, P.; Schindler, K. M.; Theobald, A.; Fritzsche,

V.; Bradshaw, A. M.; Davis, R.; Woodruff, D. P. Coverage-Dependent Changes in the Adsorption Geometry of Benzene on Ni{111}. *Surf. Sci.* **1996**, *348*, 89–99.

(47) Yamagishi, S.; Jenkins, S. J.; King, D. A. Symmetry and Site Selectivity in Molecular Chemisorption: Benzene on Ni{111}. *J. Chem. Phys.* **2001**, *114*, 5765–5773.

(48) Ihm, H.; Ajo, H. M.; Gottfried, J. M.; Bera, P.; Campbell, C. T. Calorimetric Measurement of the Heat of Adsorption of Benzene on Pt(111). *J. Phys. Chem. B* **2004**, *108*, 14627–14633.

(49) Jasen, P. V.; González, E. a.; Brizuela, G.; Juan, A. A Bonding Study of CO-Benzene Co-Adsorption on Rh(1 1 1). *J. Mol. Catal. A Chem.* **2010**, *323*, 23–27.

(50) Lin, R. F.; Koestner, R. J.; Van Hove, M. A.; Somorjai, G. A. The Adsorption of Benzene and Naphthalene on the Rh(111) Surface: A LEED, AES and TDS Study. *Surf. Sci. Lett.* **1983**, *134*, 161–183.

(51) Koel, B. E.; Somorjai, G. A. Vibrational Spectroscopy Using HREELS of Benzene Adsorbed on the Rh(111) Crystal Surface. *J. Electron Spectros. Relat. Phenomena* **1983**, *29*, 287–292.

(52) Mate, C. M.; Somorjai, G. A. Carbon Monoxide Induced Ordering of Benzene on Pt (111) and Rh (111) Crystal Surfaces. *Surf. Sci.* **1985**, *160*, 542–560.

(53) Lin, R. F.; Blackman, G. S.; Van Hove, M. A.; Somorjai, G. A. LEED Intensity Analysis of the Structure of Coadsorbed Benzene and CO on Rh(111). *Acta Crystallogr. Sect. B Struct. Sci.* **1987**, *43*, 368–376.

(54) Mate, C. M.; Somorjai, G. A.; Tom, H. W. K.; Zhu, X. D.; Shen, Y. R. Vibrational and Electronic Spectroscopy of Pyridine and Benzene Adsorbed on the Rh(111) Crystal Surface. *J. Chem. Phys.* **1988**, *88*, 441–450.

(55) Barbieri, A.; Van Hove, M. A.; Somorjai, G. A. Benzene Coadsorbed with CO on Pd(111) and Rh(111): Detailed Molecular Distortions and Induced Substrate Relaxations. *Surf. Sci.* **1994**, *306*, 261–268.

(56) Mate, C. M.; Kao, C.-T.; Somorjai, G. A. Carbon Monoxide Induced Ordering of Adsorbates on the Rh(111) Crystal Surface Importance of Surface Dipole Moments. *Surf. Sci.* **1988**, *206*, 145–168.

(57) Ohtani, H.; Wilson, R.; Chiang, S.; Mate, C. Scanning Tunneling Microscopy Observations of Benzene Molecules on the Rh(111)-(3×3) (C6H6+2CO) Surface. *Phys. Rev. Lett.* **1988**, *60*, 2398–2401.

(58) Sautet, P.; Joachim, C. Calculation of the Benzene on Rhodium STM Images. *Chem. Phys. Lett.* **1991**, *185*, 23–30.

(59) Jasen, P. V; Brizuela, G.; Padin, Z.; Gonzalez, E. a; Juan, A. Benzene and Carbon Monoxide Co-Adsorption on Pt(111): A Theoretical Study. *Appl. Surf. Sci.* **2004**, *236*, 394–405.

(60) Gonzalez, E. A.; Jasen, P. V.; Pierini, J.; Brizuela, G.; Juan, A. The Co-Adsorption of Benzene and CO on Co(0001). *Surf. Rev. Lett.* **2009**, *16*, 749–755.

(61) Habermehl-Ćwirzeń, K.; Lahtinen, J.; Hautojärvi, P. Coadsorption of CO and C6H6 on Co(0001). *Surf. Sci.* **2005**, *584*, 70–76.

(62) Stichler, M.; Weimar, R.; Menzel, D. The Influence of Electronegative Coadsorbates on the Geometry of Benzene on Ru(001). *Surf. Sci.* **1997**, *384*, 179–191.

(63) Jasen, P. V.; Gonzalez, E. A.; Juan, A.; Brizuela, G. Benzene and NO on a Ru(001) Surface: Electronic Structure and Bonding. *Appl. Surf. Sci.* **2006**, *252*, 2108–2114.

(64) Blöchl, P. E. Projector Augmented-Wave Method. *Phys. Rev. B* **1994**, *50*, 17953–17979.

(65) Kresse, G.; Joubert, D. From Ultrasoft Pseudopotentials to the Projector Augmented-Wave Method. *Phys. Rev. B* **1999**, *59*, 1758–1775.

(66) Kresse, G.; Furthmüller, J. Efficient Iterative Schemes for Ab Initio Total-Energy Calculations Using a Plane-Wave Basis Set. *Phys. Rev. B* **1996**, *54*, 11169–11186.

(67) Kresse, G.; Furthmüller, J. Efficiency of Ab-Initio Total Energy Calculations for Metals and Semiconductors Using a Plane-Wave Basis Set. *Comput. Mater. Sci.* **1996**, *6*, 15–50.

(68) Tersoff, J.; Hamann, D. Theory and Application for the Scanning Tunneling Microscope. *Phys. Rev. Lett.* **1983**, *50*, 1998–2001.

(69) Tersoff, J.; Hamann, D. R. Theory of the Scanning Tunneling Microscope. *Phys. Rev. B* **1985**, *31*, 805–813.

(70) Yildirim, H.; Greber, T.; Kara, A. Trends in Adsorption Characteristics of Benzene on Transition Metal Surfaces: Role of Surface Chemistry and van Der Waals Interactions. *J. Phys. Chem. C* **2013**, *117*, 20572–20583.

(71) Liu, W.; Ruiz, V. G.; Zhang, G. X.; Santra, B.; Ren, X.; Scheffler, M.; Tkatchenko, A. Structure and Energetics of Benzene Adsorbed on Transition-Metal Surfaces: Density-Functional Theory with van Der Waals Interactions Including Collective Substrate Response. *New J. Phys.* **2013**, *15*, 053046.

(72) Garrido Torres, J. A.; Ramberger, B.; Früchtl, H. A.; Schaub, R.; Kresse, G. Adsorption Energies of Benzene on Close Packed Transition Metal Surfaces Using the Random Phase Approximation. *Phys. Rev. Mater.* **2017**, *1*, 060803.

Graphical ToC